ARL-TR-91-14

Copy No. 1

EXPERIMENTAL DETECTION OF A SLOW ACOUSTIC WAVE IN SEDIMENT AT SHALLOW GRAZING ANGLES

Final Report under Contract N00039-88-C-0043, TD No. 01A044, Bottom Penetration at Shallow Grazing Angles

Frank A. Boyle
Nicholas P. Chotiros

APPLIED RESEARCH LABORATORIES
THE UNIVERSITY OF TEXAS AT AUSTIN
POST OFFICE BOX 8029, AUSTIN, TEXAS 78713-8029

24 May 1991

Final Report

Prepared for:

NAVAL OCEANOGRAPHIC AND
ATMOSPHERIC RESEARCH LABORATORY
STENNIS SPACE CENTER, MS 39529-5004

Monitored by:

SPACE AND NAVAL WARFARE SYSTEMS COMMAND
DEPARTMENT OF THE NAVY
WASHINGTON, D.C. 20363-5100

DISCLAIMER NOTICE

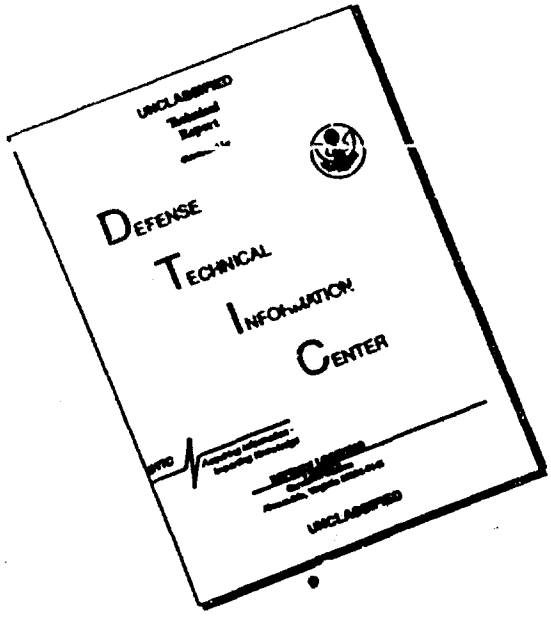

THIS DOCUMENT IS BEST QUALITY AVAILABLE. THE COPY FURNISHED TO DTIC CONTAINED A SIGNIFICANT NUMBER OF PAGES WHICH DO NOT REPRODUCE LEGIBLY.

REPORT DOCUMENTATION PAGE

Form Approved
OMB No. 0704-0188

1. AGENCY USE ONLY (Leave blank)	2. REPORT DATE	3. REPORT TYPE AND DATES COVERED
	24 May 91	final, 2 Feb 90 - 31 Jan 91

4. TITLE AND SUBTITLE
Experimental Detection of a Slow Acoustic Wave in Sediment at Shallow Grazing Angles, Final Report under Contract N00039-88-C-0043, TD No. 01A044, Bottom Penetration at Shallow Grazing Angles

5. FUNDING NUMBERS
N00039-88-C-0043
TD No. 01A044

6. AUTHOR(S)
Boyle, Frank A. Chotiros, Nicholas P.

7. PERFORMING ORGANIZATION NAMES(S) AND ADDRESS(ES)
Applied Research Laboratories
The University of Texas at Austin
P.O. Box 8029
Austin, Texas 78713-8029

8. PERFORMING ORGANIZATION REPORT NUMBER
ARL-TR-91-14

9. SPONSORING/MONITORING AGENCY NAME(S) AND ADDRESS(ES)
Naval Oceanographic and Atmospheric Research Laboratory
Stennis Space Center, Mississippi 39529-5004

Space and Naval Warfare Systems Command
Department of the Navy
Washington, D.C. 20363-5100

10. SPONSORING MONITORING AGENCY REPORT NUMBER

11. SUPPLEMENTARY NOTES

12a. DISTRIBUTION/AVAILABILITY STATEMENT

12b. DISTRIBUTION CODE

13. ABSTRACT (Maximum 200 words)

Following recent experimental results at sea (N.P. Chotiros, Proceedings of Ocean '89) that suggest the existence of a previously undetected type of acoustic wave in sandy sediments, an experiment was designed to detect and measure the speed of acoustic waves in an isolated environment. The experiment was conducted in a laboratory tank containing 1 m of unwashed river sediment under a 3 m water column. Observations were made of the travel time and attenuation of a pulse from an acoustic source located above the water-sediment interface to a set of probes below the interface. It was observed that at normal incidence the pulse traveled at about 1675 m/s, while at shallow grazing angles the pulse traveled through the sediment at close to 1200 m/s.

An interesting possible explanation exists in the Biot theory for acoustic propagation through fluid-saturated porous media which predicts a slow acoustic wave in porous materials. The Biot model predicts wavespeeds close to those
(see reverse side)

14. SUBJECT TERMS
backscatter, Biot, evanescent wave, frame bulk modulus, gassy sediment, grain bulk modulus, grazing angle, porous medium, reflection coefficient, sediment, shear wave

15. NUMBER OF PAGES
41

16. PRICE CODE

17. SECURITY CLASSIFICATION OF REPORT	18. SECURITY CLASSIFICATION OF THIS PAGE	19. SECURITY CLASSIFICATION OF ABSTRACT	20. LIMITATION OF ABSTRACT
UNCLASSIFIED	UNCLASSIFIED	UNCLASSIFIED	SAR

13. (cont'd)

observed, given a particular set of input parameters. Since the actual values of these parameters have not been measured and are not well known, it is not possible to draw conclusions about the applicability of the Biot model at the present time. Studies were also made of the effect of gas content on the acoustic properties predicted by the Biot model. It was concluded that gas content affects acoustic properties significantly and must be accounted for in any theoretical models to be developed.

TABLE OF CONTENTS

LIST OF FIGURES

LIST OF TABLES

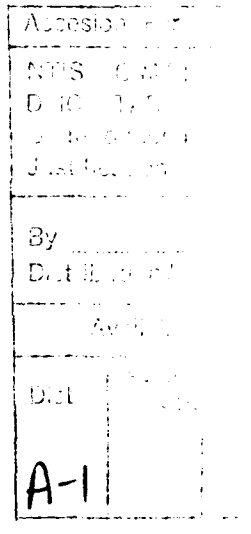

Statement A per telecon Richard Root
NOARL/Code 112
Stennis Space Center, MS 39529-5004

NWW 9/26/91

PREFACE

This final report covers the work that Applied Research Laboratories was tasked to perform under Contract N00039-88-C-0043, TD No. 01A044.0, entitled Bottom Penetration at Shallow Grazing Angles

EXECUTIVE SUMMARY

This work was conducted under the project bottom penetration at shallow grazing angles. The objective is a new theory of acoustic bottom penetration and backscatter to account for recent experimental observations.

An experiment was performed in a laboratory tank with 1 m of unwashed river sediment under a 3 m water column. A vertical array of hydrophones was positioned in the sediment. A projector was positioned 0.5 m above the sediment interface. It was mounted on a rolling platform so that the projector's horizontal position could be adjusted. Measurements of the arrival times of signals at each hydrophone from the projector were taken and compared with Snell's law calculations, based on the expected speed of sound in the water and the sediment.

It was found that, at near-normal incidence, propagation times matched those predicted by the Snell's law calculations. At shallow grazing angles the propagation times suggested the existence of a new kind of propagation: one with a significantly slower sound speed. These results are consistent with earlier experiments by Chotiros at Kings Bay, South Carolina, and Panama City, Florida.

The existence of such a wave is predicted by the Biot theory for acoustic propagation in fluid-filled porous media. The Biot theory differs from other commonly used models in that it treats the sediment as a two-phase medium; it is a porous skeletal structure through which a separate fluid component flows freely, rather than simply a single phase viscoelastic fluid or a solid. An interesting prediction from the Biot theory is the existence of two compressional acoustic waves. For the faster of these waves, the fluid component moves in phase with the solid skeletal structure. It is similar to the common compressional wave that propagates through a solid. In the slow wave, the fluid component oscillates out of phase with the solid skeletal structure. This wave usually attenuates rapidly and is difficult to detect. To the authors' knowledge, Biot slow waves have not previously been detected in natural sandy sediments.

In order to conclude that the results described here are due to the Biot slow wave, further study is required concerning several input parameters upon which the Biot wave speeds and attenuations depend. Several of these parameters are difficult to measure and have not been satisfactorily determined. It was found that one can get the Biot model to predict our experimental results by varying these input parameters appropriately.

Additionally the effect of gas content within the sediment needs to be studied. By combining the Biot model with a model developed by Hawkins (ARL:UT) on the properties of gassy fluids, some simple calculations were made of reflection coefficients and wave speeds as functions of gas content. Significant dependance of these wave speeds and reflection coefficients on gas content was observed.

These results have important implications not only for high frequency acoustic bottom penetration, but also for shallow water propagation models over a wide band of frequencies. They indicate the existence of penetration and forward reflection loss mechanisms that are not accounted for in the current models.

1. INTRODUCTION

This work was conducted under the project bottom penetration at shallow grazing angles (TD No. 01A044). The objective is a new theory of acoustic bottom penetration and backscatter to account for recent experimental observations.

In recent years there has been considerable interest in acoustic propagation through sandy sediment. It is noteworthy that current theoretical models do not always predict experimental observations well. Muir *et al.*[1] performed an experiment wherein a 20 kHz acoustic beam was incident upon a sediment surface from a water column above. When the signal was incident on sediment at a shallow grazing angle, unexpected complications were found that were attributed to a bottom interaction. Williams *et al.*[2] performed some measurements of a similar beam and compared the resulting pressure fields in the sediment with theory. Observations were generally consistent, except at subcritical grazing angles. In these cases the pressure fields bore little resemblance to those predicted by theory.

In 1989 Chotiros[3,4] summarized the results of some acoustic penetration experiments at sea. In these experiments signals broadcast from atop underwater towers were measured by hydrophones buried at various depths and locations around the towers. It was found that, at shallow grazing angles, sound speeds and attenuations were not well modeled by current theories, which treat the sediment as either a fluid or solid medium.

The speed of sound in the sediment had been measured prior to each of Chotiros' experiments and was near 1742 m/s. Since this speed is faster than the speed of sound in the water column above, acoustic wavefronts from the water are expected to behave as in Fig. 1.1, wherein the wavefront bends up toward the boundary upon refraction. Associated with this refraction is a critical grazing angle. A wavefront incident at less than the critical grazing angle will experience total internal reflection back up into the water column above, leaving no refracted energy in the sediment.

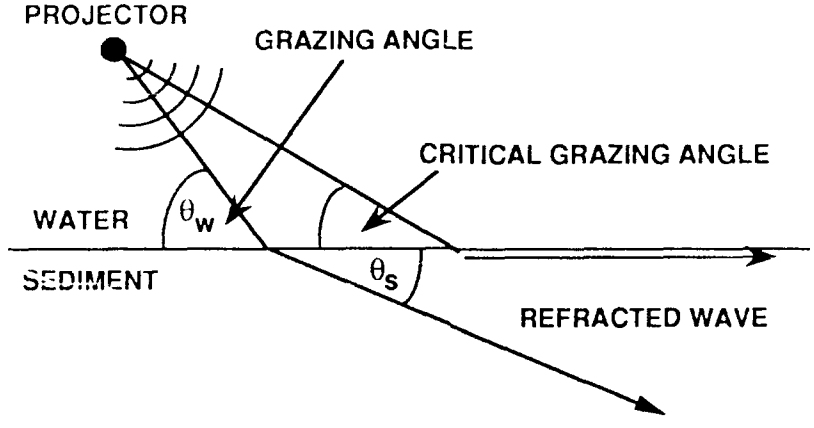

FIGURE 1.1
PATH OF REFRACTED ACOUSTIC SIGNAL FOR $c_w < c_s$

ARL:UT
AS-91-261
FAB - GA
6-12-91 Cnt1

Chotiros found a significant amount of acoustic energy deep in the sediment, even when the incident wavefront was at a grazing angle below critical. Furthermore, the wavefronts in the sediment associated with this energy seemed to propagate at close to 1200 m/s. He suggested that a previously undetected type of acoustic propagation may exist, one with a sediment sound speed of about 1200 m/s. If such a wave does exist, it should refract at the interface as in Fig. 1.2. No critical grazing angle exists for this type of refraction.

An experiment was designed and conducted in the ARL:UT tank laboratory to detect and measure the speed of these slow acoustic waves in an isolated environment, as described in Section 2. A slow wave was clearly detected at shallow grazing angles. A possible explanation in terms of Biot's theory is given in Section 3. Our conclusions and plans for further work are given in Sections 4 and 5.

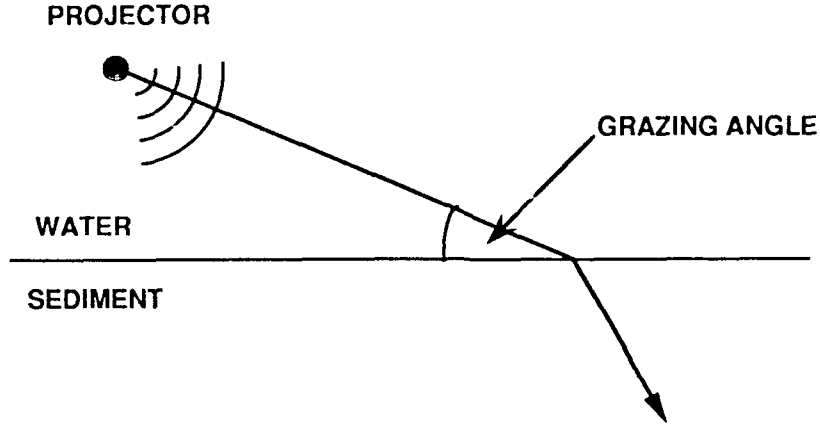

FIGURE 1.2
PATH OF REFRACTED ACOUSTIC SIGNAL FOR $c_w > c_s$

2. LABORATORY TANK EXPERIMENT

2.1 PROCEDURE

Our apparatus is illustrated in Fig. 2.1. This laboratory tank, constructed 18 years ago for earlier research, measures 18.29 m long, 4.57 m wide, and 3.65 m deep. The tank contains 1 m of unwashed river sediment under a 3 m water column. The sediment had been slowly poured through the water column and allowed to settle. A collection of hydrophones were then buried at various depths. Over the tank was a motorized platform which could be moved to any position along the length of the tank. Attached to this platform was a vertical column on the bottom of which was mounted an acoustic projector. A data collection sequence consisted of (1) positioning the platform to a specific location along the length of the tank, (2) insonifying the buried hydrophones with a short acoustic pulse from the projector, and (3) sampling the signals from each buried hydrophone for 6 ms. A complete collection of data consisted of about 225 such data collection sequences taken at incremental locations along the length of the tank.

The experiment was managed on a Macintosh computer through a Labview interface. The computer generated a periodic trigger which was sent to a signal generator that created a short pulse for the acoustic projector to transmit. The timeseries signals from each buried hydrophone were amplified, filtered, converted from analog to digital, and returned to the Macintosh disk for later analysis.

Of critical importance to our experiment is the flatness of the water-sediment interface in our tank. We measured it to be flat to within a 1.8 cm standard deviation, with no measurable mean gradient from one end of the tank to the other. We took data at wavelengths (in water) as short as 2.5 cm. At small grazing angles, the vertical component of the wavelength is large in comparison with the variation in height of the sediment. We therefore treated the interface as a flat surface.

We used two types of pulses. One was a two cycle pulse at 60 kHz. The other was one cycle at 30 kHz. The signals were generated by an Exact Electronics signal generator and amplified to get a peak current of 5 A through

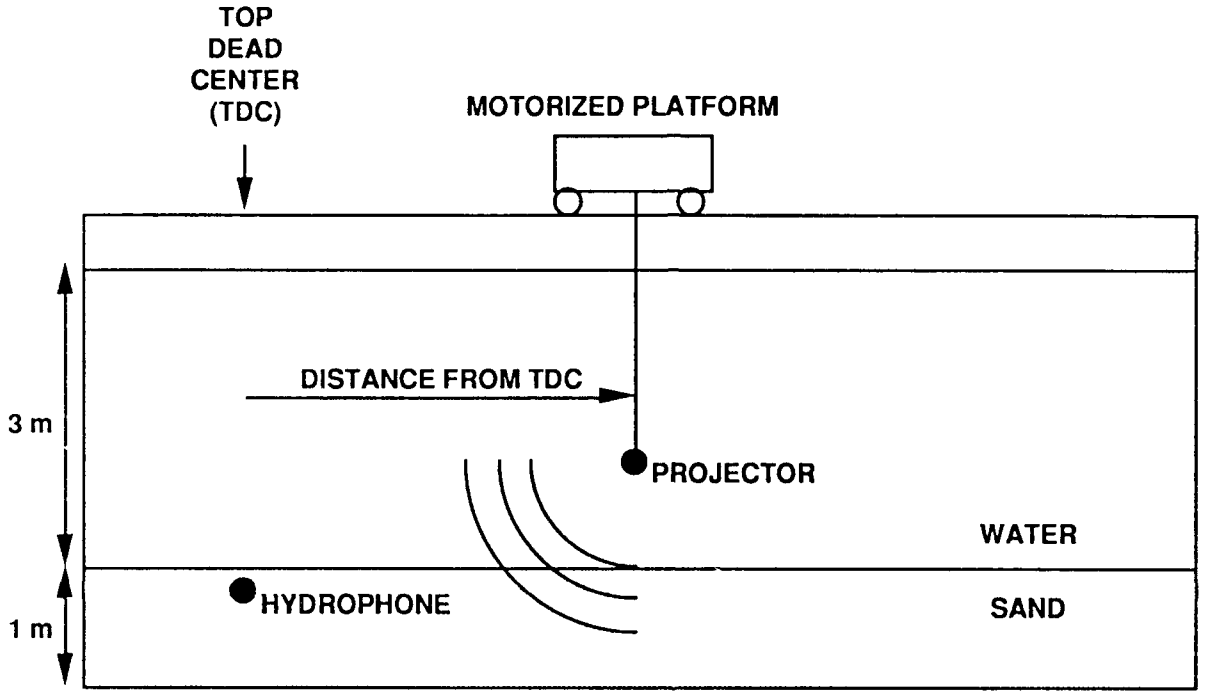

FIGURE 2.1
TANK EXPERIMENT
THE PLATFORM ROLLS ALONG RAILS ON OPPOSITE SIDES OF THE TANK. AT DISCRETE LOCATIONS, THE PROJECTOR INSONIFIES THE ARRAY OF BURIED PROBES WITH A SHORT PULSE. THE RESULTING ACOUSTIC SIGNAL AT EACH PROBE IS RECORDED.

ARL:UT
AS-91-263
FAB - GA
6-12-91 Crt1

the projector. This was the maximum current allowed by the TR 225 projector. We computed our source level at 191 dB re 1 μPa at 1 m. This appears to have been generally adequate for producing a measurable signal-to-noise ratio at the buried receivers, even at very shallow grazing angles. The data were processed via Hilbert transform so that the envelope of the signal from each probe could be displayed.

2.2 RESULTS

The data from each buried hydrophone were presented for analysis as described in Fig. 2.1 and shown in Figs. 2.2 - 2.5. The vertical axis represents the time delay after transmission. The horizontal axis is the horizontal position of the projector along the length of the tank. The colors represent the acoustic intensity measured by a buried hydrophone. Each data collection sequence is represented by a thin vertical strip, on which acoustic intensity is plotted against time delay. When all the data are presented, a narrow bright curve of peak acoustic intensity is apparent. This curve is an experimental plot of the pulse travel time measured by the buried hydrophone as a function of the horizontal position of the projector. The delay time is a minimum when the projector is directly over the hydrophone, a position we call top dead center.

Figure 2.2 shows the data measured by a probe at the water-sediment interface. Overlaid onto the data in black is a plot of the theoretical prediction of the pulse travel time as a function of projector position along the length of the tank. This prediction is based on the known speed of sound in the water. The experimental data and the prediction line up well, thus providing a confidence check of the calibrations involved.

Figure 2.3 shows the data as measured by a hydrophone buried 8 cm deep in the sediment. Overlaid onto these data are three curves that represent different predicted travel times of the pulse at the hydrophone, based on three models of acoustic propagation in the sediment. The bottom curve is a Snell's law calculation for a refracted wave, based on the known speed of sound in the water of 1489 m/s and a sediment sound speed of 1675 m/s, consistent with

CONTINUED ON PAGE 17

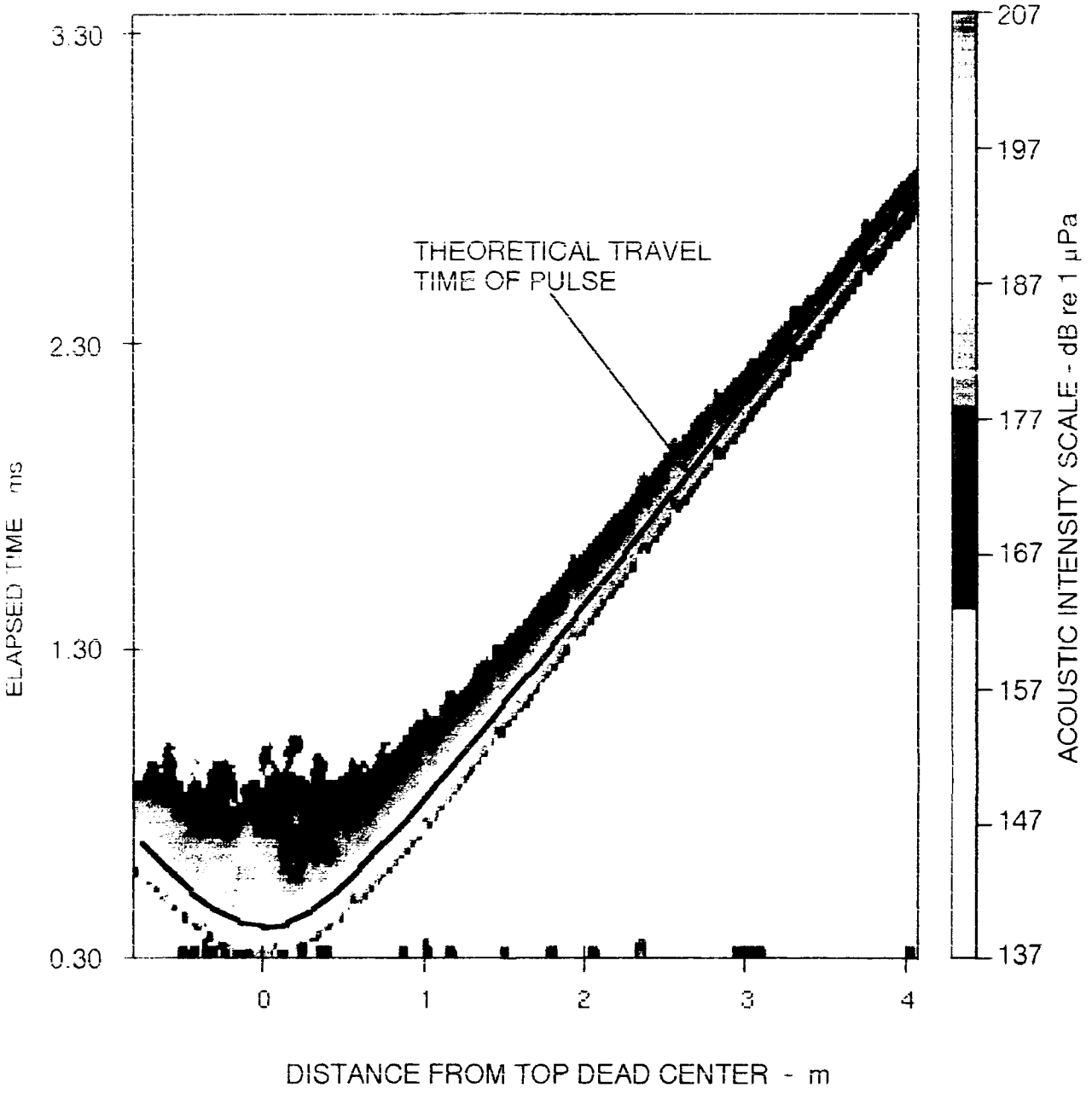

FIGURE 2.2
ACOUSTIC INTENSITY AS A FUNCTION OF PROJECTOR DISTANCE FROM TOP DEAD CENTER AND ELAPSED TIME SINCE PULSE GENERATION, PROBE ON THE WATER-SEDIMENT INTERFACE

ARL:UT
AS-91-264
FAB - GA
6-12-91 Crt1

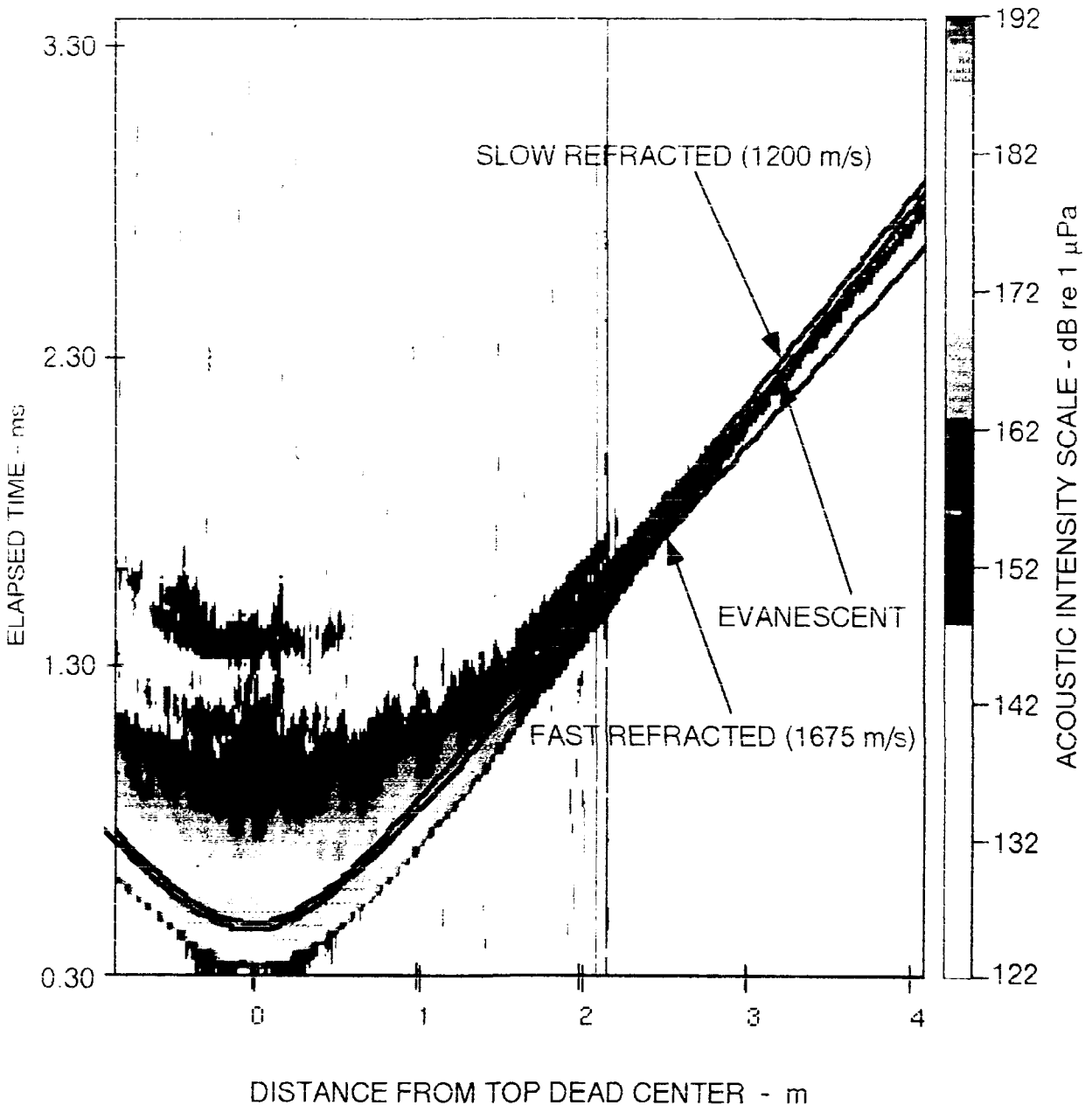

FIGURE 2.3
ACOUSTIC INTENSITY AS A FUNCTION OF PROJECTOR DISTANCE FROM TOP DEAD CENTER AND ELAPSED TIME SINCE PULSE GENERATION, PROBE BURIED .080 m BELOW SEDIMENT INTERFACE

ARL:UT
AS-91-265
FAB - GA
6-12-91 Crt1

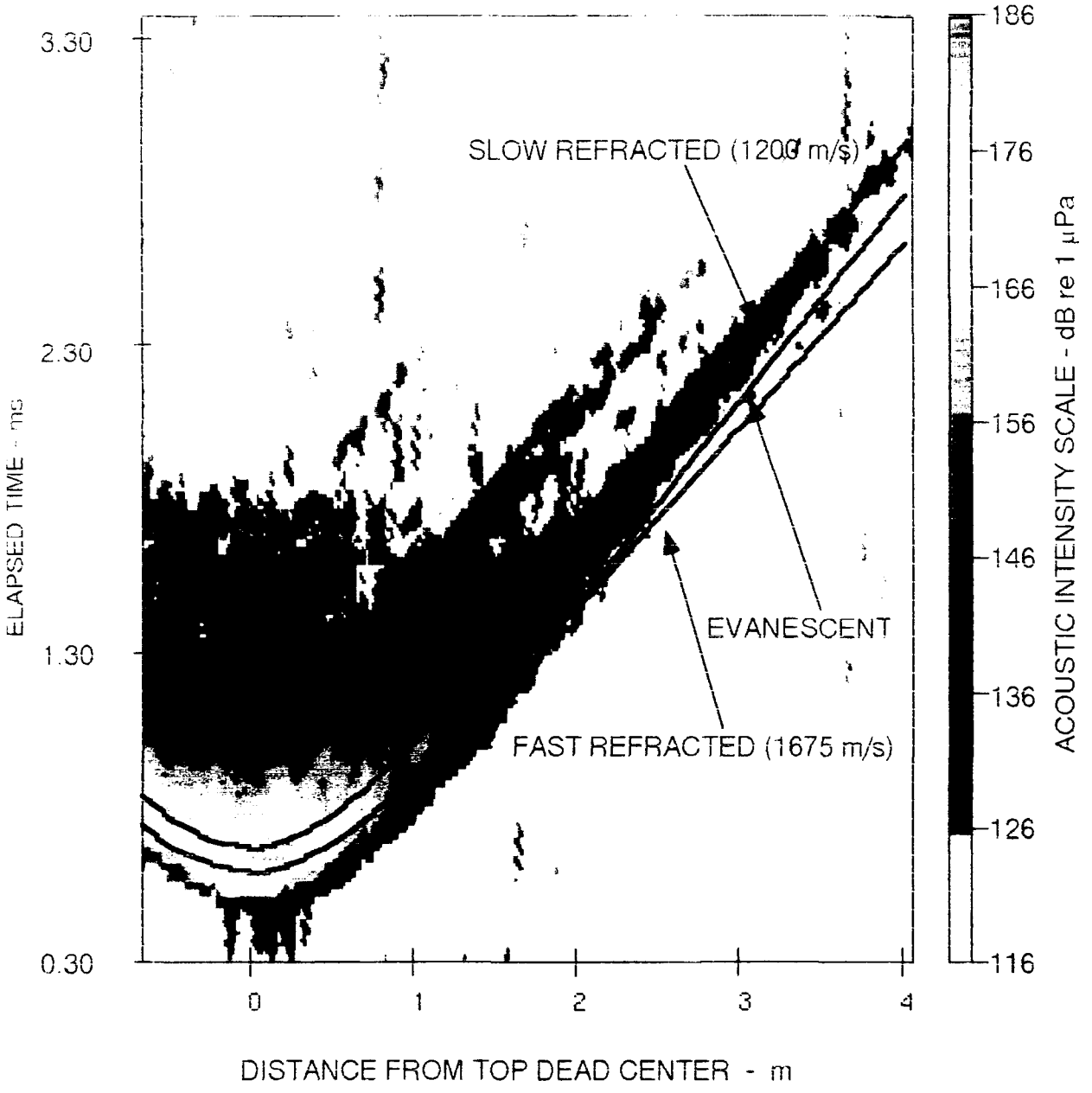

FIGURE 2.4
ACOUSTIC INTENSITY AS A FUNCTION OF PROJECTOR DISTANCE FROM TOP DEAD CENTER AND ELAPSED TIME SINCE PULSE GENERATION, PROBE BURIED .330 m BELOW SEDIMENT INTERFACE

ARL:UT
AS-91-266
FAB - GA
6-12-91 Crt1

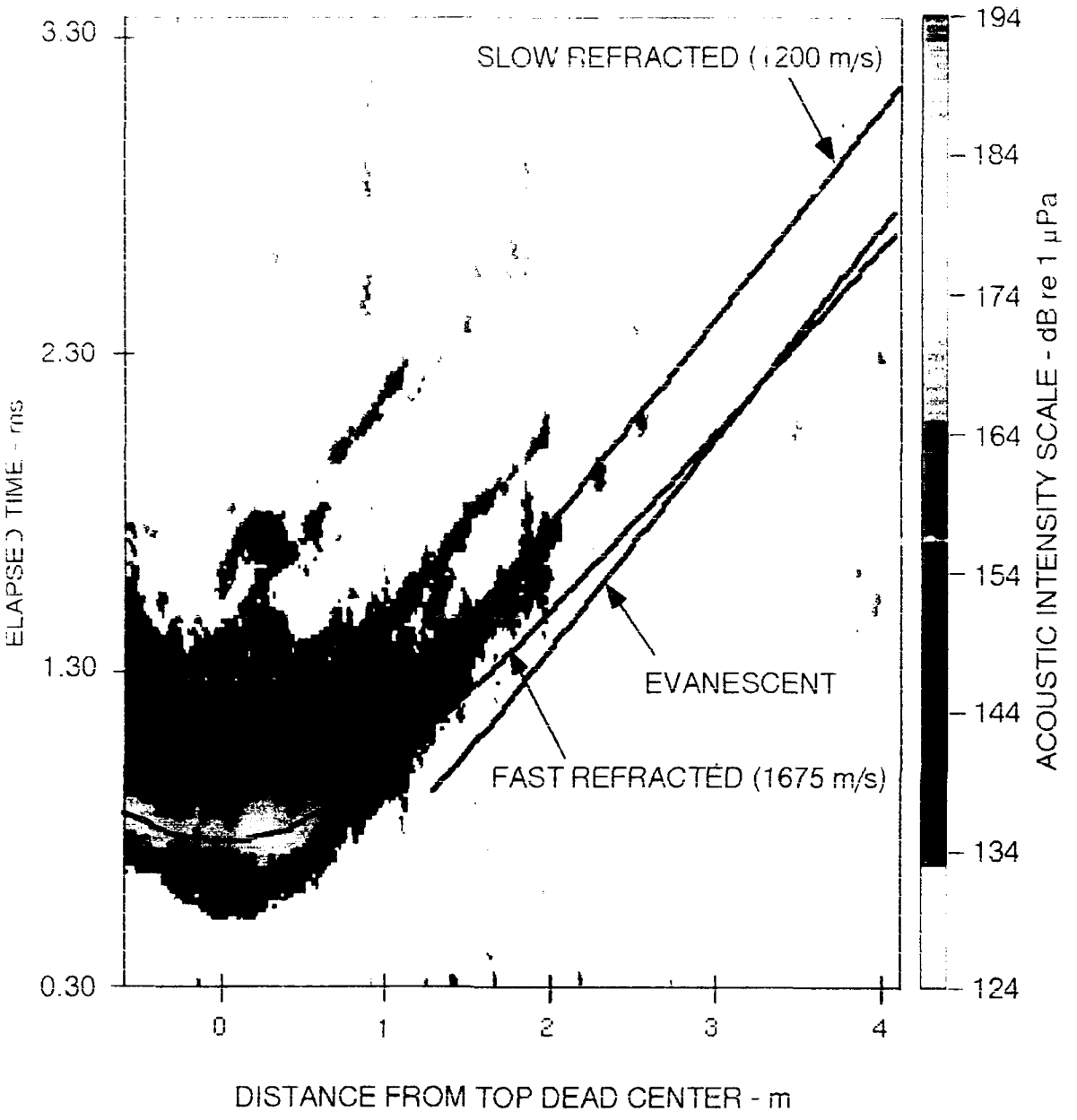

FIGURE 2.5
ACOUSTIC INTENSITY AS A FUNCTION OF PROJECTOR DISTANCE FROM TOP DEAD CENTER AND ELAPSED TIME SINCE PULSE GENERATION, PROBE BURIED .614 m BELOW SEDIMENT INTERFACE

ARL:UT
AS-91-267
FAB - GA
6-12-91 Crt1

earlier measurements in the tank.[1] It will be called the "fast refracted" model. The middle curve shows the predicted arrival of an evanescent wave at a point on the interface directly above the hydrophone. This will be called the "evanescent" model. The top curve is another Snell's law prediction, wherein the sediment sound speed is assumed to be 1200 m/s, the "slow refracted" model.

At normal incidence the fast refracted model is in good agreement with experimental observations. As the horizontal separation between the projector and receiver increases, the observed arrival times favor either the evanescent or the 1200 m/s refracted wave. It is difficult to distinguish between these two models at this depth.

Figures 2.4 and 2.5 show the data as measured by hydrophones at 33 cm and 61 cm below the interface, respectively. Overlaid onto the data are the models for fast refracted, evanescent, and slow refracted waves. The arrival times are generally well modeled by the fast refracted wave at near-normal incidence, whereas at shallower grazing angles the slow refracted model clearly fits the data best.

The data presented were from a 2 cycle 60 kHz pulse input to the projector, with bandpass filtering between 50 and 70 kHz at the receivers. Data was also collected using a 30 kHz pulse. The latter results, not shown, generally exhibited the same kind of behavior, though signals were considerably weaker in comparison with background noise.

2.3 DISCUSSION

The observed arrival times at shallow grazing angles appear to favor the slow refracted model. We consider a few possible explanations for this.

One possible explanation is that the sediment might be an anisotropic medium; because the sediment was slowly sifted into the tank and allowed to settle there could be some horizontal stratification. If the speed of sound in the horizontal direction differed significantly from that in the vertical direction, our results might be explainable. Specifically, if the horizontal speed of sound were

near 1200 m/s, our data would be consistent. The horizontal sound speed in the tank, however, has been measured at 1669 ±83 m/s.

Another possibility is ducting in narrow horizontal channels in the sediment. It could be that the abovementioned measurement of horizontal sound speed was outside such a channel and thus failed to detect any slow propagation. The observed 1200 m/s acoustic wave might then be the result of slow effective propagation through a duct. This explanation seems unlikely in the light of the fact that the same 1200 m/s acoustic waves were observed by receivers at several different depths.

It is not likely that the 1200 m/s wave is a shear wave. Shear waves have been measured for sandy sediments similar to that in our tank, and generally travel at less than 150 m/s, an order of magnitude slower.[5-7]

3. BIOT MODEL

3.1 BIOT THEORY

An interesting possible explanation for the effects we are seeing is offered by the Biot[8-11] theory for acoustic propagation in fluid-filled porous media. Generally, other models used to describe the sediment are single phase models, assuming either a solid or viscoelastic fluid type of medium. The Biot theory applies to a medium that consists of a solid skeletal frame, through which a fluid component is allowed to flow freely. Biot derived the following coupled pair of differential equations that govern the displacements of the fluid and solid components.

$$N\nabla^2\mathbf{u} + \text{grad}\,[(A+N)e + Q\varepsilon] = \frac{\partial^2}{\partial t^2}\left((\rho_1+\rho_{12})\mathbf{u} + \rho_{12}\mathbf{U}\right)$$

$$\text{grad}\,[Qe + R\varepsilon] = \frac{\partial^2}{\partial t^2}\left(\rho_{12}\mathbf{u} + (\rho_{12}+\rho_2)\mathbf{U}\right) \quad ,$$

where

U	= fluid displacement vector,
u	= solid displacement vector,
e	= div **u**,
ε	= div **U**,
N	= shear modulus,
A,Q,R	= constants,
ρ_1	= mass of solid / unit volume,
ρ_2	= mass of fluid / unit volume, and
ρ_{12}	= solid-fluid coupling coefficient.

By performing certain operations on this pair of equations, it is possible to derive the acoustic properties of the medium. For example, by taking the curl of both sides of both equations, one can arrive at a wave equation that describes the propagation of shear waves. By taking the divergence of both equations

one can find a coupled pair of wave equations that govern the propagation of compressional waves.

It is interesting that the Biot theory predicts two compressional waves. The faster of these is a wave wherein the fluid moves in phase with the solid frame that defines the porous medium. This wave is usually dominant and corresponds to the common compressional wave that travels through an ordinary solid medium. The slower wave usually attenuates rapidly and has not, to the authors' knowledge, previously been detected in natural sandy sediments.

According to the Biot model, an incident acoustic wave from the water to the sediment will excite three refracted waves at the boundary, as in Fig. 3.1. If the wavefront is incident at below the critical angle for this fast refracted wave, the fast wave will not exist in the sediment, allowing the slow and shear waves to dominate. Wu *et al.*[12] demonstrated that, for a synthetic material made of fused glass beads, the transmission coefficients for the Biot waves were sensitive to the grazing angle. At greater than the critical angle, the transmission coefficient for the fast wave was much greater than that for the slow wave. At grazing angles less than critical, the fast wave's transmission coefficient vanished, whereas that for the slow wave increased. If the sediment in our experiment behaves similarly, this could explain why the fast refracted model is applicable at near-normal incidence, whereas the slow wave fits best at shallow grazing angles.

3.2 BIOT MODEL COMPARISON WITH EXPERIMENT

In order to use the Biot model as a possible explanation for the apparent slow acoustic propagation, one must determine what wave speeds the Biot model predicts. One of the difficulties in using the Biot model is its sensitive dependence on input parameters that are not well defined or easily measured. Stern *et al.*[13] and Stoll *et al.*[14] collected values for all of the parameters that were believed to characterize typical sandy sediments. By applying Stern's values, listed in Table 3.1, to the Biot model, one obtains the sound speed curves in Fig. 3.2. In this plot, the predicted Biot wave speeds are displayed as

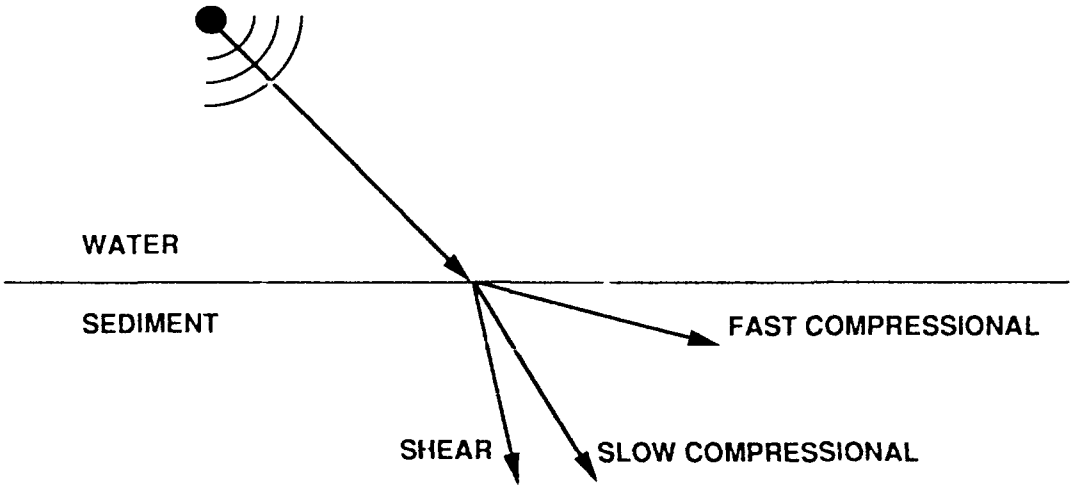

FIGURE 3.1
EXCITATION OF THE THREE BIOT WAVES AT THE BOUNDARY

TABLE 3.1

BIOT INPUT PARAMETERS FROM STERN, 1985

fluid density	1000	kg/m^3
fluid bulk modulus	2.0×10^9	μPa
porosity	0.47	
grain density	2650	kg/m^3
pore size parameter	1.0×10^{-5}	m
viscosity	1.0×10^{-3}	kg/m-s
permeability	1.0×10^{-10}	m^2
grain bulk modulus	3.6×10^{10}	μPa
frame shear modulus	2.61×10^7	μPa
shear logarithmic decrement	0.15	
frame bulk modulus	4.36×10^8	μPa
bulk logarithmic decrement	0.15	
gas bulk modulus	2.48×10^5	

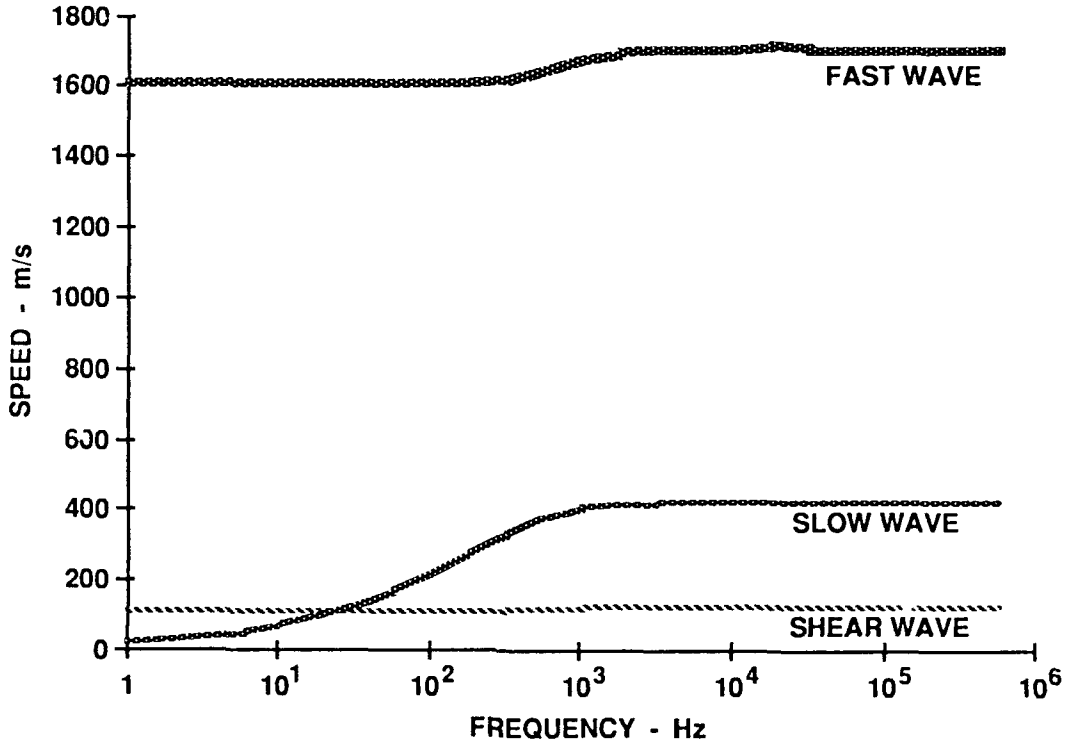

FIGURE 3.2
BIOT MODEL WAVE SPEEDS USING PARAMETERS FROM STERN, 1985 (TABLE 3.1)

a function of frequency. At our experimental frequencies of 30 and 60 kHz, Biot fast and slow waves are predicted to be 1700 m/s and 500 m/s, respectively.

At first glance the above data does not seem to model our experimental results very well. One must consider, however, that some of the input parameters are difficult to measure accurately. The Biot wave speeds sometimes depend quite sensitively on these parameters. Some of these parameters are the porosity and the bulk and shear moduli of the individual grains as well as of the solid skeletal frame of the porous medium. In Fig. 3.3 the same calculation as in Fig. 3.2 was carried out, with the exception that two parameters were modified in such a way that the predicted wave speeds match those observed experimentally. These modified input parameters are listed in Table 3.2. The two parameters changed were grain and frame bulk moduli. The grain bulk modulus was reduced by a factor of 4 from the value for perfect quartz crystals, and the frame bulk modulus was increased by a factor of 10 from Stern's assumed value. Since the true values of neither are known, and both are difficult to measure, there is no evidence to contradict our assumed values. Furthermore, our assumed values are not improbable for the following reasons. Due to imperfections, one should expect the grain bulk modulus of sand to be less than that of perfect quartz crystals. Due to consolidation over an extended period, the frame bulk modulus may well be as high as our assumed value.

3.3 THE EFFECT OF GAS CONTENT

The compressibility of the fluid phase of the medium is another ill-defined parameter. Its value will depend on the presence of gas within the sediment. The Biot wave speeds will depend on its value, and therefore on gas content. Some investigation on the effects of gas content was made using a theoretical model developed by Hawkins *et al.*[15] Hawkins' model was employed to adjust the effective fluid density and bulk modulus, given a particular gas fraction and bubble size distribution. These input parameters were then applied to the Biot model. The Biot wave speeds depended sensitively on gas content, as is illustrated in Fig. 3.4, where Biot wave speeds are plotted against gas

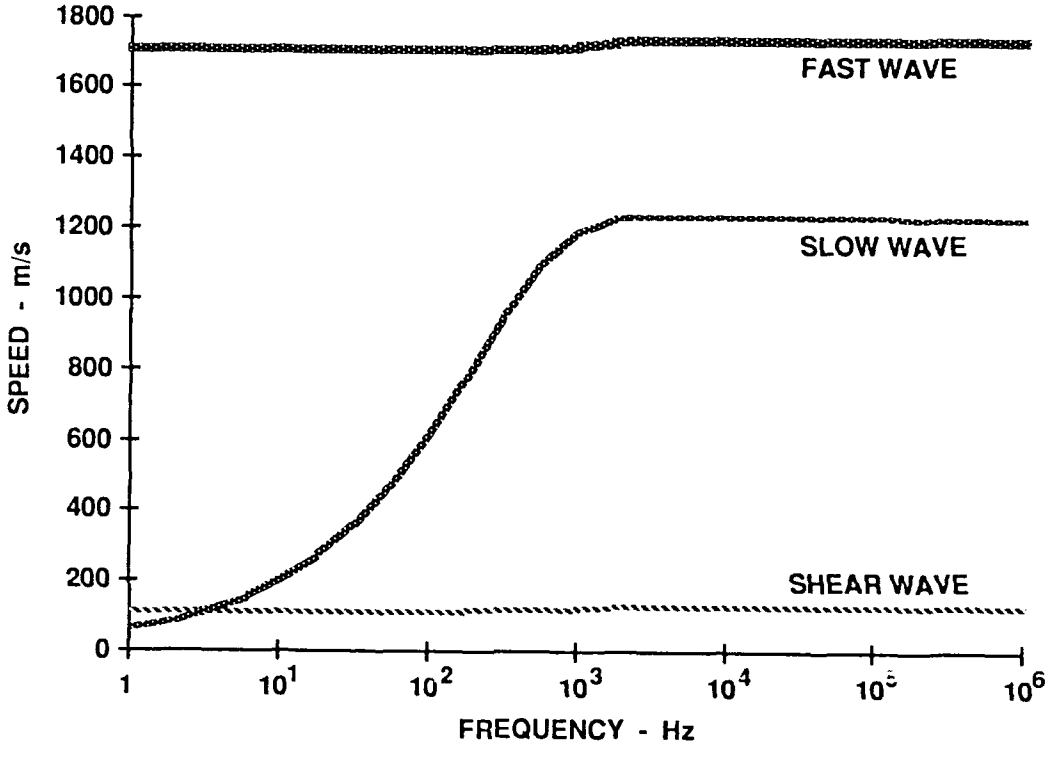

FIGURE 3.3
BIOT WAVE SPEEDS versus FREQUENCY,
MODIFIED BIOT PARAMETERS (TABLE 3.2)

TABLE 3.2

MODIFIED BIOT INPUT PARAMETERS

fluid density	1000	kg/m^3
fluid bulk modulus	2.0×10^9	μPa
porosity	0.47	
grain density	2650	kg/m^3
pore size parameter	1.0×10^{-5}	m
viscosity	1.0×10^{-3}	kg/m-s
permeability	1.0×10^{-10}	m^2
grain bulk modulus	0.9×10^{10}	μPa
frame shear modulus	2.61×10^7	μPa
shear logarithmic decrement	0.15	
frame bulk modulus	4.36×10^9	μPa
bulk logarithmic decrement	0.15	
gas bulk modulus	2.48×10^5	

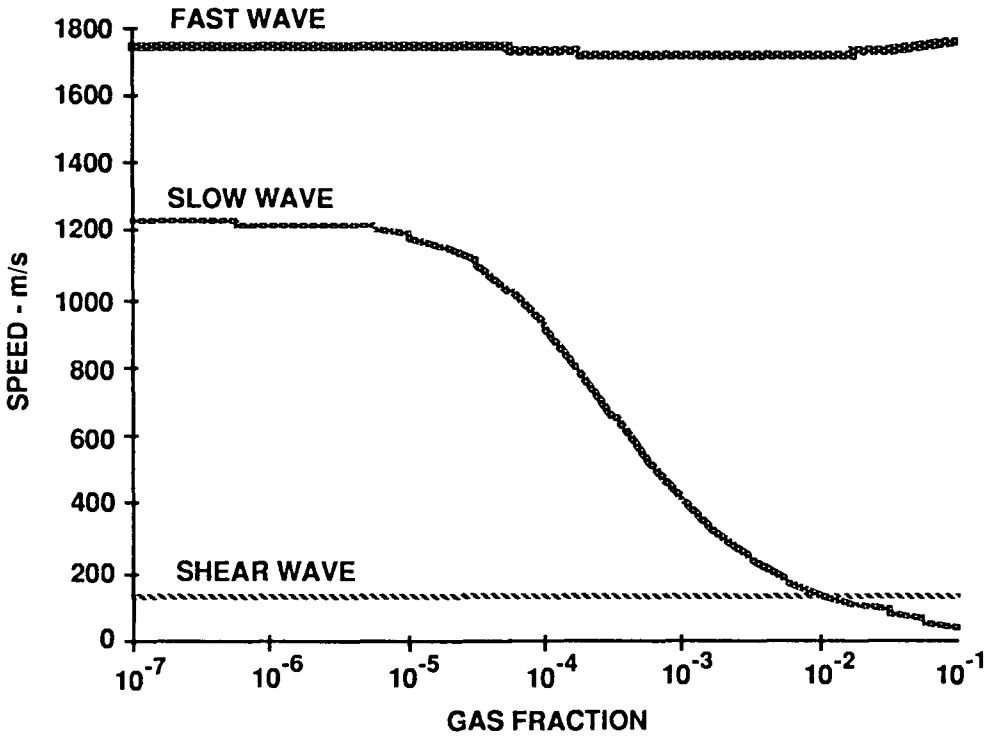

FIGURE 3.4
BIOT WAVE SPEEDS versus GAS CONTENT,
MODIFIED BIOT PARAMETERS (TABLE 3.2)

content. Since bubble radius should be comparable to pore radius, the mean bubble radius for this plot was assumed equal to the pore size parameter.

Studies were also made of reflection and transmission coefficients as functions of gas content. Some simple calculations of these coefficients were made with Hawkins' model and the Biot theory as described above. Figure 3.5 is a plot of the reflection coefficient as a function of gas fraction and frequency. Noteworthy is a broad minimum in the reflection coefficient of 100 Hz - 100 kHz when the gas fraction is between 10^{-3} and 10^{-5}. No corresponding peak in the transmission coefficient was observed. This broad minimum may have important implications for propagation models over a wide band of frequencies.

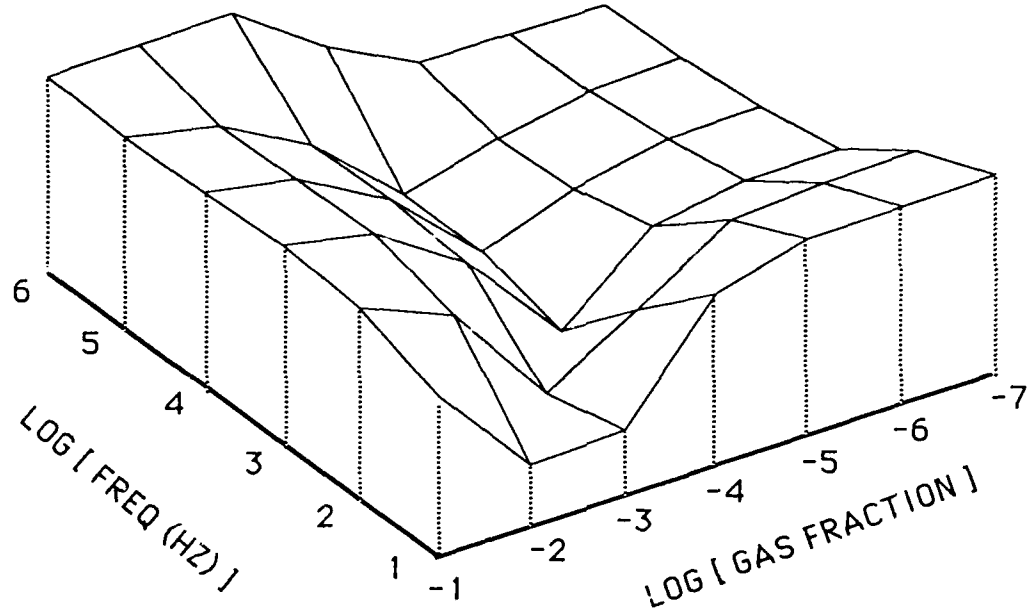

	LOG [GAS FRACTION]						
LOG [FREQ (HZ)]	-7	-6	-5	-4	-3	-2	-1
1	0.9125	0.9114	0.9011	0.8021	0.3493	0.3319	0.7611
2	0.7841	0.7815	0.7551	0.5030	0.2759	0.7494	0.9202
3	0.5644	0.5583	0.4988	0.1787	0.6139	0.8669	0.9583
4	0.5105	0.5025	0.4316	0.2870	0.6523	0.8752	0.9607
5	0.4918	0.4840	0.4161	0.3053	0.6616	0.8783	0.9616
6	0.4907	0.4923	0.5082	0.7163	0.9970	0.9971	0.9979

FIGURE 3.5
REFLECTION COEFFICIENT versus FREQUENCY
AND GAS CONTENT, MODIFIED BIOT PARAMETERS
(TABLE 3.2)

4. CONCLUSIONS

Based on the observations in this experiment as well as those performed previously by Chotiros, the authors conclude that a slow acoustic wave has been observed. This conclusion has important implications for ocean bottom backscatter modeling and for shallow water forward propagation modeling. The Biot model is the most likely explanation of the nature of this slow wave. Before any conclusions can be made regarding the applicability of the Biot model, further studies concerning Biot input parameters will be required.

Gas content has a significant effect on sound speeds predicted by the Biot model. It will have to be accounted for in any theoretical models to be developed.

5. PLANS FOR FURTHER WORK

Our plans are to determine if Biot's theory can satisfactorily account for the slow wave phenomenon. The most direct approach is to develop experimental techniques to measure the unknown Biot parameters. Of particular interest are experimental techniques that might be designed to independently measure the frame bulk modulus, grain bulk modulus, and gas content. With a more precise knowledge of these quantities, one will be able to determine the nature of the observed slow acoustic wave and make theoretical predictions about its behavior.

Following the measurement of the Biot parameters we plan to investigate the effect of trapped gas bubbles both on the transmission properties of a sandy sediment and on the backscattering strength at shallow grazing angles. These studies will fill a substantial gap in the currently used theoretical models. A theoretical model will be developed and compared with experimental data for verification.

REFERENCES

1. T. G. Muir, C. W. Horton, Sr., and L. A. Thompson, "The Penetration of Highly Directional Acoustic Beams into Sediments," J. Sound Vib. **64**, 539-551 (1979).

2. K. L. Williams, L. J. Satkowiak, and D. R. Bugler, "Linear and Parametric Array Transmission across a Water-Sand Interface - Theory, Experiment, and Observation of Beam Displacement," J. Acoust. Soc. Am. **86** (1), 311-325 (1989).

3. N. P. Chotiros, "High Frequency Acoustic Bottom Penetration: Theory and Experiment," Proceedings of Oceans '89, Vol. 4. (IEEE Publication No. 89CH2780-5).

4. N. P. Chotiros, "High Frequency Acoustic Penetration Analysis," Applied Research Laboratories Technical Report No. 89-28 (ARL-TR-89-28), The University of Texas at Austin, 1989.

5. R. D. Stoll, G. M. Bryan, R. Flood, D. Chayes, and P. Manley, "Shallow Seismic Experiments Using Shear Waves," J. Acoust. Soc. Am. **83** (1), 93-102 (1988).

6. R. D. Stoll, "Theoretical Aspects of Sound Transmission in Sediments," J. Acoust. Soc. Am. **68** (5), 1341-1349 (1980).

7. R. D. Stoll, Lecture Notes in Earth Sciences, Vol. 26: Sediment Acoustics (Springer-Verlag, Berlin, Heidelberg, 1989).

8. M. A. Biot, "Theory of Propagation of Elastic Waves in a Fluid-Saturated Porous Solid. I. Low Frequency Range," J. Acoust. Soc. Am. **28**, 168-178 (1956).

9. M. A. Biot, "Theory of Propagation of Elastic Waves in a Fluid-Saturated Porous Solid. II. Higher Frequency Range," J. Acoust. Soc. Am. **28**, 179-191 (1956).

10. M. A. Biot, "Mechanics of Deformation and Acoustic Propagation in Porous Media," J. Appl. Phys. **33**, 1482-1498 (1962).

11. M. A. Biot, "Generalized Theory of Acoustic Propagation in Porous Dissipative Media," J. Acoust. Soc. Am. **34**, 1254-1264 (1962).

12. K. Wu, Q. Xue, and L. Adler, "Reflection and Transmission of Elastic Waves from a Fluid-Saturated Porous Solid Boundary," J. Acoust. Soc. Am. **87** (6), 2349-2358 (1990).

13. M. Stern, A. Bedford, and H. R. Millwater, "Wave Reflection from a Sediment Layer with Depth-Dependent Properties," J. Acoust. Soc. Am. **77** (5), 1781-1788 (1985).

14. R. D. Stoll, "Marine Sediment Acoustics," J. Acoust. Soc. Am. **77** (5), 1789-1799 (1985).

15. J. A. Hawkins, Jr., and A. Bedford, "A Variational Model for Bubbly Liquids: Reflection from a Liquid-Bubbly Liquid Interface," Presentation at 120th Meeting of the Acoustical Society of America, J. Acoust. Soc. Am. **88** (Suppl. 1), S131 (1990).

24 May 1991

DISTRIBUTION LIST FOR
ARL-TR-91-14
FINAL REPORT UNDER CONTRACT N00039-88-C-0043,
TD No. 01A044, Bottom Penetration at Shallow Grazing Angles

Copy No.		
	Commanding Officer	
	Naval Oceanographic and Atmospheric Research Laboratory	
	Stennis Space Center, MS 39529-5004	
1	Attn:	R. Farwell (Code 240)
2		D. Young (Code 333)
3		P. Fleischer (Code 361)
4		K. Briggs (Code 333)
5		P. Valent (Code 310)
6		R. Love (Code 243)
7		B. Adams (Code 113)
8		E. Franchi (Code 200)
9		S. Stanic (Code 243)
10 - 21		Library (Code 125L)
	Office of Naval Technology	
	Department of the Navy	
	Arlington, VA 22217-5000	
22	Attn:	W. Ching (Code 235)
23		T. Goldsberry (Code 231)
	Commanding Officer	
	Naval Oceanographic Office	
	Stennis Space Center, MS 39522-5000	
24	Attn:	W. Jobst (Code OA)
25		J. Bunce (Code OW)
26		R. Christensen (Code OAR)
27		E. Beeson (Code OARR)
	Office of Naval Research Detachment	
	Stennis Space Center, MS 39529-5004	
28	Attn:	B. Blumenthal (ONR DET 125)
29		E. Chaika (ONR DET 125)
	Commander	
	Naval Oceanography Command	
	Stennis Space Center, MS 39522-5000	
30	Attn:	D. Durham (Code N5A)

Distribution List for ARL-TR-91-14 under Contract N00039-88-C-0043,
TD No. 01A044
(cont'd)

Copy No.

Commander
Naval Sea Systems Command
Department of the Navy
Washington, DC 20362-5101

31 Attn: J. Grembi (PMS407B)
32 D. Gaarde (PMS407D4)
33 J. Neely (PMS418W)
34 T. Douglass (PMS402B)
35 H. Grunin (PMS402)
36 A. Knobler (PMS406B)

Office of the Chief of Naval Operations
Department of the Navy
Washington, DC 20360

37 Attn: R. Widmayer (OP 374T)
38 R. Winokur (OP 096T)
39 K. Martello (OP 954F1)
40 T. Fraim (OP 986G)
41 R. James (OP 006DX)
42 H. Montgomery (OP 9878)
43 J. Boosman (OP 987J)

Commander
Mine Warfare Command
Charleston Naval Base
Charleston, SC 29408

44 Attn: G. Pollitt (Code N4A)
45 B. O'Connel (Code N3A)

Commanding Officer
Naval Coastal Systems Center
Panama City, FL 32407

46 Attn: D. Folds (Code 20C)
47 R. Johnson (Code 210T)
48 D. Todoroff (Code 2120)
49 L. Flax (Code 210)

Distribution List for ARL-TR-91-14 under Contract N00039-88-C-0043, TD No. 01A044
(cont'd)

Copy No.

Officer in Charge
Naval Underwater Systems Center
New London Laboratory
New London, CT 06320-5594

50 Attn: W. Roderick (Code 33A3)
51 J. Geary (Code 3221)
52 W. Cary (Code 33A)
53 J. Chester (Code 3331)
54 P. Koenig (Code 3331)

Officer in Charge
Naval Underwater Systems Center
Newport Laboratory
Newport, RI 02841-5047

55 Attn: J. Kelly (Code 3632)
56 F. Aidala (Code 362)
57 W. Gozdz (Code 36291)

Office of the Chief of Naval Research
Department of the Navy
Arlington, VA 22217-5000

58 Attn: R. Obrochta (Code 1125OA)
59 J. Kravitz (Code 1125GG)
60 M. Orr (Code 11250A)
61 K. Lackie (Code 125)
62 D. Houser (Code 232)
63 A. Faulstich (Code 23)

Commanding Officer
Naval Ocean Systems Center
San Diego, CA 92152

64 Attn: R. Anderson (Code 54)

Commanding Officer
Naval Surface Warfare Center
White Oak Laboratory
Silver Spring, MD 20910

65 Attn: S. Martin (Code U24)
66 J. Sherman (Code U20)
67 M. Stripling (Code U04)

Distribution List for ARL-TR-91-14 under Contract N00039-88-C-0043,
TD No. 01A044
(cont'd)

Copy No.

	Commanding Officer Naval Surface Warfare Center Dahlgren Laboratory Dahlgren, VA 22448
68	Attn: S. Burgess (NGM Library)
69 - 80	Commanding Officer and Director Defense Technical Information Center Cameron Station, Building 5 5010 Duke Street Alexandria, VA 22314
	Applied Physics Laboratory The University of Washington 1013 NE 40th Street Seattle, WA 98105
81	Attn: D. Jackson
82	Library
	Applied Research Laboratory The Pennsylvania State University P. O. Box 30 State College, PA 16804
83	Attn: S. McDaniel
84	D. McCammon
85	F. Symons
86	J. Beebe
87	D. Upshaw
88	E. Liszka
89	Library
	Presearch, Inc. 8500 Executive Park Avenue Fairfax, VA 22031
90 - 92	Attn: J. R. Blouin
	The University of Texas at Austin Physics Department Austin, TX 78712
93	Attn: W. D. McCormick
94	M. Fink
95	T. Griffy

Distribution List for ARL-TR-91-14 under Contract N00039-88-C-0043,
TD No. 01A044
(cont'd)

Copy No.	
	The University of Texas at Austin Aerospace Engineering Department Austin, TX 78712
96	Attn: M. Bedford
97	Robert A. Altenburg, ARL:UT
98	Hollis Boehme, ARL:UT
99	Frank A. Boyle, ARL:UT
100	Nicholas P. Chotiros, ARL:UT
101	John M. Huckabay, ARL:UT
102	T. G. Muir, ARL:UT
103	Robert A. Stewart, ARL:UT
104 - 109	Library, ARL:UT
110 - 115	Reserve, ARL:UT